Electronic Supplementary Material (ESI) for Energy & Environmental Science.

– Supplementary Information –

A photosystem I monolayer with anisotropic electron flow enables Z-scheme like photosynthetic water splitting

Fangyuan Zhao,[a] Panpan Wang,[a] Adrian Ruff,[a] Volker Hartmann,[b] Sónia Zacarias,[c] Inês. A. C. Pereira,[c] Marc M. Nowaczyk,[b] Matthias Rögner,[b] Felipe Conzuelo*[a] and Wolfgang Schuhmann*[a]

[a] *Analytical Chemistry - Center for Electrochemical Sciences (CES), Faculty of Chemistry and Biochemistry, Ruhr University Bochum, Universitätsstr. 150, D-44780 Bochum, Germany*

[b] *Plant Biochemistry, Faculty of Biology and Biotechnology, Ruhr University Bochum, Universitätsstr. 150, D-44780 Bochum, Germany*

[c] *Instituto de Tecnologia Química e Biológica António Xavier, Universidade Nova de Lisboa, Oeiras 2780-157, Portugal*

* Corresponding authors

Tel.: +49 234 32 26200; fax: +49 234 32 14683

e-mail: wolfgang.schuhmann@rub.de, felipe.conzuelo@rub.de

Synthesis and Characterization of P-vio

Materials and Methods

All chemicals and materials for the synthesis of P-vio and the corresponding precursors were purchased from Sigma-Aldrich, Alfa Aesar, VWR, Merck, Fluka or J.T Baker and were of analytical grade or higher and were used as received except otherwise noted. The deuterated solvents acetone-d_6 and DMSO-d_6 were purchased from Euriso-top and were stored at 4 °C or room temperature, respectively. Dry dimethylformamide was purchased from Acros-organics and was stored over molecular sieves in AcroSeal bottles. All aqueous solutions including electrolytes were prepared with deionized water from a Milli Q water purification system. The synthesis of 1-methyl-[4,4']-bipyridinium iodide (**1**), the monomer 3-azido-propyl methacrylate (N_3MA) and the polymer backbone poly(3-azido-propyl methacrylate-*co*-butyl acrylate-*co*-glycidyl methacrylate) (P(N_3MA-BA-GMA)) was described in ref. [1]. All reactions and manipulations under inert conditions were conducted by using the Schlenk technique.

All NMR experiments were conducted at 300 K with a Bruker DPX200 spectrometer with a proton resonance frequency of 200.13 MHz. The residual solvent peak was used as internal standard. UV-Vis spectrometric measurements were carried out with an Agilent Cary60 spectrophotometer in quartz or polystyrene cuvettes with an optical path length of 1 cm. All absorption spectra were background corrected. FT-IR measurements (reflection mode) were measured with a Nicolet iN10 FT-IR microscope from Thermo Scientific. Samples were drop cast from acetone or water onto a silver wafer and dried at air or at 45 °C (20 min to 30 min), respectively, prior to experiments. ESI-MS experiments were conducted with an LTQ-Orbitrap XL spectrometer from Thermo Fisher Scientific. Samples were dissolved in acetonitrile.

Electrochemical Experiments

All electrochemical experiments for the characterization of the freely diffusing viologen unit (**2**) and the redox polymer P-vio were performed with a conventional three electrode cell under argon atmosphere at room temperature. As reference electrode a Ag/AgCl/3 M KCl system was employed. As counter electrode a Pt wire was used. As working electrodes graphite disk electrodes (3 mm or 4 mm diameter) or glassy carbon (3 mm diameter) were used. For measurements with the redox polymer, the material was drop cast onto the electrode surface and dried at room temperature prior to the experiment. Cyclic voltammograms were recorded with scan rates between 20 mV s^{-1} and 100 mV s^{-1}, and were not background corrected. Working electrodes were polished following standard protocols prior to each experiment.

Syntheses

The synthesis of the alkyne terminated viologen modified **2** and the attachment of **2** to the N_3-modifed co-polymer backbone P(N_3MA-BA-GMA) (Scheme S1) were conducted following protocols described earlier in ref.[1]. The actual composition of the polymer backbone was previously determined by means of ^{1}H-NMR spectroscopy to be N_3MA = 71 mol%, BA = 20 mol% and GMA = 9 mol% (nominal composition: N_3MA = 80 mol%, BA = 10 mol%, GMA = 10 mol%).[1]

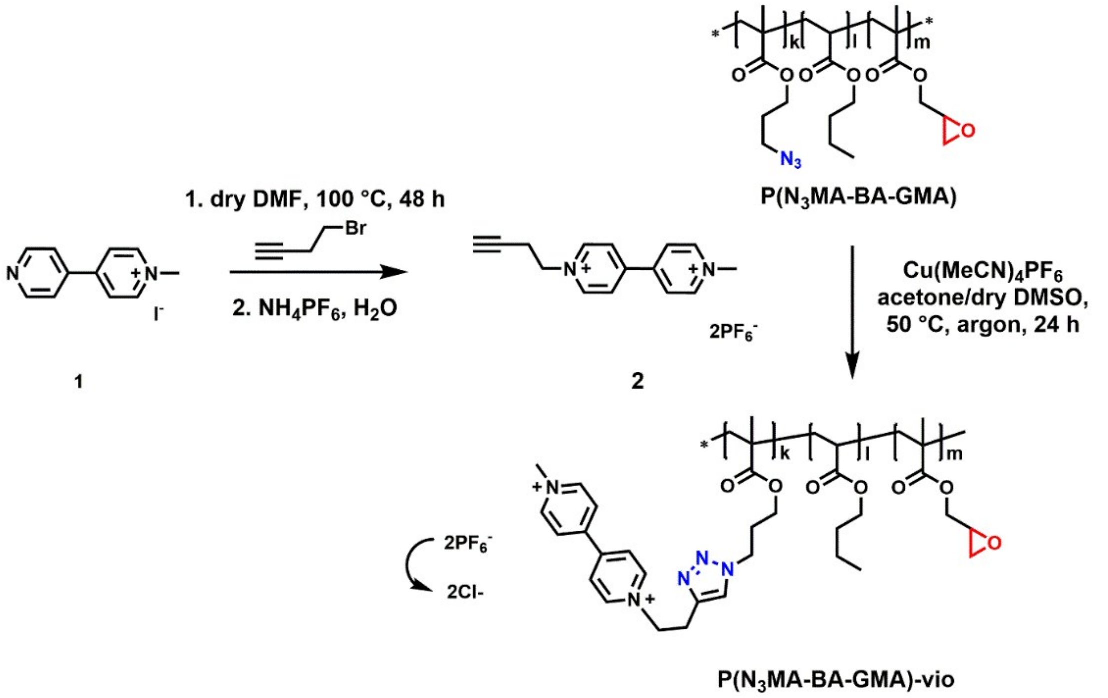

Scheme S1. Multistep synthesis of the redox polymer P-vio. The alkyne terminated viologen based modifier was prepared via an alkylation reaction of **1** with 4-bromo-1-butyne in dry DMF. Metathesis reaction with NH_4PF_6 leads to the PF_6^--salt of **2**. The latter was bound to the polymer backbone P(N_3MA-BA-GMA) in a click chemistry approach using a 1,3-dipolar cycloaddition between the terminal alkyne in **2** and the azide group (blue) within the copolymer backbone to yield the redox polymer P-vio with a quantitative conversion rate. Exchange of the hydrophobic PF_6^- counterions against the more hydrophilic Cl^- anions via dialysis leads to the formation of an aqueous polymer solution. The electrophilic epoxide functions (red) within the redox polymer can be used as anchoring sites for crosslinking reaction with nucleophilic crosslinkers, e.g., dithiols or diamines. Crosslinking further enhances the film stability on the electrode surface.

*Synthesis of N-butynyl-N'-methyl-[4,4']-bipyridinium bis(hexafluorophosphate) (**2**)*

Under argon atmosphere, the bipyridine precursor 1-methyl-[4,4']-bipyridinium iodide (1 g, 3.36 mmol) was dissolved in 15 mL of dry dimethylformamide. Then, a slight excess of 4-bromo-1-alkyne (410 µL, 4.36 mmol) was added and the mixture was stirred at 100 °C for 48 h under argon atmosphere. The red slurry was cooled down to room temperature and the formed precipitate was filtered off. The residue was washed with 150 mL of ethyl acetate and air dried. The crude product was re-dissolved in 15 mL of water and quenched with 18 mL of an aqueous 1 M NH_4PF_6 solution. The slurry was stored in the fridge overnight to complete the precipitation. The colourless precipitate was filtered off and washed with cold water. The residue was finally dried under reduced pressure to yield 976 mg (56%) of a colourless powder. ^{1}H-NMR (200.13 MHz, acetone-d_6) δ/ppm: 9.50 and 9.47 (s, 2H, aromatic protons), 9.38 and 9.35 (s, 2H, aromatic protons), 8.83-8.92 (multiple signals, 4H, aromatic protons), 5.13 (t, $J_{H,H}$ = 6.6 Hz, 2H, =N-CH_2-CH_2-), 4.74 (s, 3H, =N-CH_3), 3.19 (td, $J_{H,H}$ = 6.6 Hz, $J_{H,H}$ = 2.6 Hz, 2H, -CH_2-C≡CH), 2.71 (t, $J_{H,H}$ = 2.6 Hz, 1H, -C≡CH). UV-Vis (DMSO) λ/nm: 265 nm (max). FT-IR (reflection mode, drop cast from acetone onto silver wafer, Fig. S1a) wavenumber/cm^{-1}: 3298, 3138, 3083 (C-H bands), 2121 (-C≡C-H), 1954, 1836, 1706, 1643 (vs, s, C-N), 1562 (s, s), 1540 (s, s), 1446 (vs, s), 1331, 805 (vs, P-F) overlapping with 772. Redox potentials of the first (E_1) and second (E_1) reduction, measured by means of solution cyclic voltammetry (Fig. S2, red trace) with the halide form (prior to metathesis reaction with NH_4PF_6) in 25 mM Tris-buffer containing 25 mM KCl at a glassy carbon electrode: $E_1 = -425$ mV vs. SHE, $E_2 = -734$ mV vs. SHE. ESI-MS (MeCN, positive ions) m/z: calculated for $[C_{15}H_{16}N_2PF_6]^+$ 369.09 (100%), 370.10 (16.2%), 371.10 (1.2%), found 369.08 (100%), 370.04 (16.5%), 371.08 (1.4%).

*Synthesis of poly(3-azido-propyl methacrylate-co-butyl acrylate-co-glycidyl methacrylate)-viologen (**P-vio**)*

In a Schlenk round bottom flask, the polymer backbone P(N_3MA-BA-GMA) (642 µL of an acetone solution with $c = 127$ g mL^{-1}, this corresponds to m(polymer) = 81.5 mg and 67.6 mg N_3MA or 0.4 mmol N_3-functions, assuming a N_3MA amount of 71 mol%/83 wt%) was dissolved under argon atmosphere in 8 mL of acetone. To this solution 2 mL of DMSO and the alkyne terminated viologen **2** (206 mg, 0.4 mmol) were added. The mixture was purged with argon to remove O_2 from the solution. Then, the copper(I) catalyst $Cu(MeCN)_4PF_6$ (149 mg, 0.4 mmol) was added in stoichiometric amounts.[2] The reaction mixture was stirred at 50 °C overnight. The solution was cooled down to room temperature followed by the addition of 20 mL of diethyl ether under stirring. The precipitate was allowed to settle down and the supernatant was decanted off. The brownish residue was washed first with 2×20 mL of diethyl ether, then with 5×10 mL of water and finally with 3×25 mL of diethyl ether again. Finally, the polymer was dried under reduced pressure to yield a pale brown powder (153.7 mg). The crude PF_6^- salt of the polymer was stored as a solid. ^{1}H-NMR (200.13 MHz, DMSO-d_6) δ/ppm: 9.2 – 9.3 (multiple signals, broad, aromatic protons of the bipyridine core), 8.71 (s, broad, aromatic protons of the bipyridine core), 7.97 (s, weak, broad, C-H of triazole unit), 4.96 (=N-CH_2-), 4.82 and 4.44 (=N-CH_3) overlapping, 1.58 and 1.23 (methylene groups), 0.84 (CH_3 of backbone), strong and broad water signal at around 3.5 ppm heavily overlaps with signal from polymer backbone. Redox potentials of the first (E_1) and second (E_1) reduction, measured by means of cyclic voltammetry (Fig. S2, blue trace) with the PF_6^- salt drop cast onto a glassy carbon electrode in 25 mM Tris-buffer containing 25 mM KCl: $E_1 = -280$ mV vs. SHE, $E_2 = -684$ mV vs. SHE.

Metathesis reaction with Cl^- and purification of P-vio by means of dialysis against aqueous KCl and water

The following protocol describes a typical procedure for anion exchange and purification of the polymer P-vio: Appropriate aliquots of the polymer were suspended in water and small amounts of DMSO followed by the addition of small amounts of aqueous KCl solutions (0.1 M to 3 M). The mixture was stirred over night to completely dissolve the polymer. Insoluble parts were discarded, and the green-yellow polymer solution was subjected to dialysis against aqueous KCl by using centrifugation and membrane filters with a molecular weight cut-off of 5 kDa (Vivaspin, Sartorius). After extensive dialysis against aqueous KCl solution the polymer was dialyzed against copious amounts of water to remove excess KCl. The purified polymer was obtained as yellowish solution and stored at room temperature or in the fridge at 4 °C. UV-Vis (DMSO) λ/nm: 265 nm (max). FT-IR (reflection mode, drop cast from water onto silver wafer and dried at 45 °C, Fig. S1b) wavenumber/cm^{-1}: 3776 (-O-H, residual water in the hydrogel matrix), 3120, 3044, 2992, 2963 (all C-H), 2101 (w, broad, residual N_3-functions), 1725 (vs, s, C=O), 1639 (s, s, C=N and C=O), 1455 (m, s) 1275 (m, s), 1232 (m, s), 1157 (vs, s) 1050 (m, s), 967 (w, s), 833 (s, s, aromatic C-H), 779, 749, 713 (all w, s).

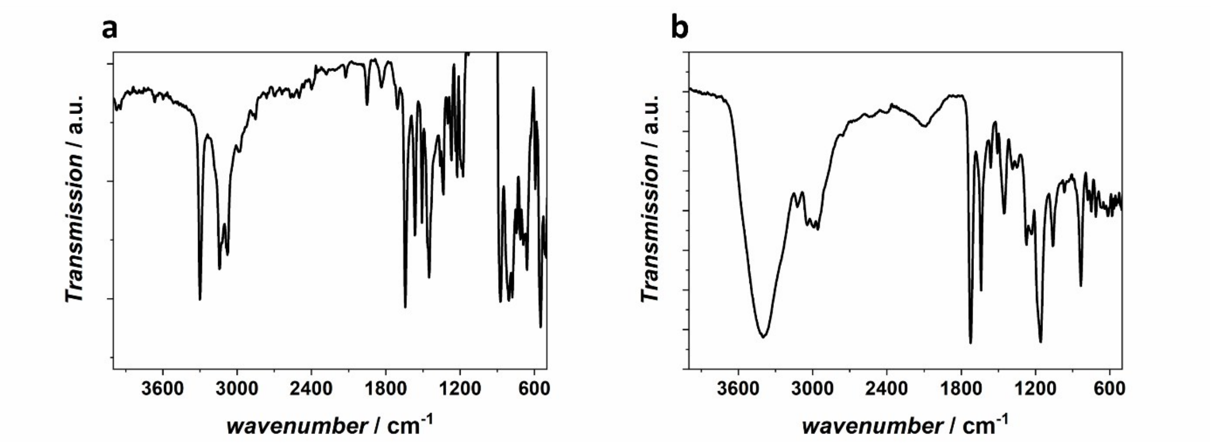

Fig. S1. FT-IR (reflection mode) characterization of the free alkyne terminated viologen **2** (a) and the redox polymer **P-vio** (b). Samples were coated onto silver wafers for measurements. The spectrum of **2** shows a band at 2121 cm^{-1} that is characteristic for the C-H mode of alkynes. The modified redox polymer shows only a weak signal at 2101 cm^{-1} that can be assigned to residual N_3-functions within the polymer backbone. Note that in the unmodified polymer the N_3-vibration band reveals similar intensity than the C=O mode located at 1725 cm^{-1}.[1] Hence, we conclude that the attachment of the viologen units to the polymer backbones proceed with almost quantitative conversion. The broad and intense signal at around 3376 cm^{-1} can be assigned to residual water entrapped in the hydrogel matrix.

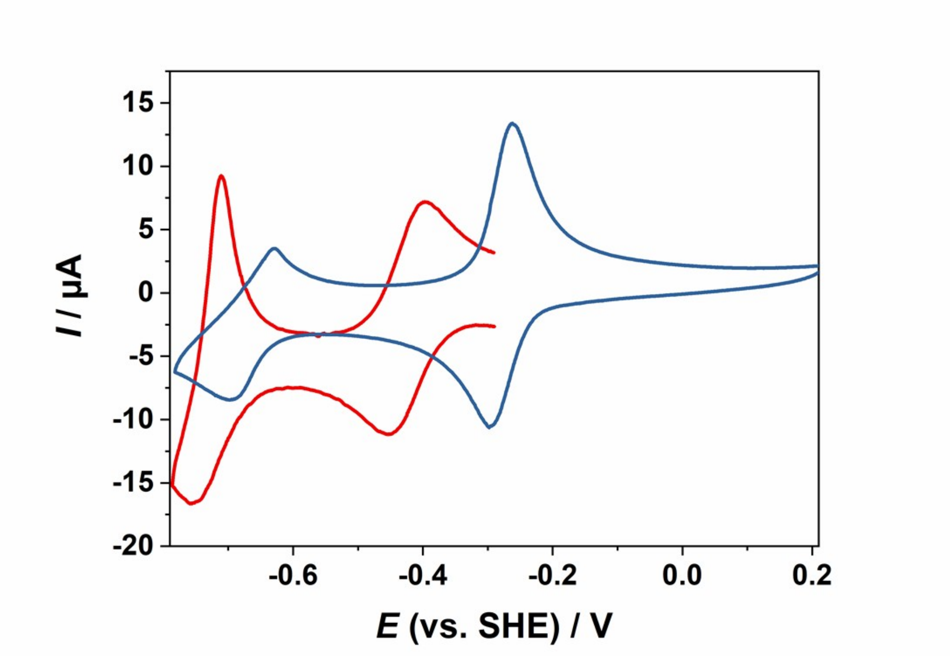

Fig. S2. Cyclic voltammetric characterization of the freely diffusing viologen **2** (red trace) and the redox polymer **P-vio** (blue trace) in 25 mM Tris-buffer containing 25 mM KCl at a glassy carbon electrode; scan rate = 100 mV s^{-1}. The unbound viologen **2** was measured as the halide salt in solution. The PF_6^- salt of the polymer was drop cast onto the electrode surface from acetone and measured as film. The midpoint potentials of the first (E_1) and second (E_2) redox processes were estimated to be $E_1 = -425$ mV vs. SHE and $E_2 = -734$ mV vs. SHE for **2** as well as $E_1 = -280$ mV vs. SHE and $E_2 = -684$ mV vs. SHE for **P-vio**. Evidently, in the polymer bound state both reduced species (radical cation and neutral form) are stabilized by the polymer matrix. The same effect as well as similar potential values were observed when a C6 (hexyne-based) instead of the here used C4 (butyne-based) linker was used for the attachment of the viologen species.[1]

Transfer of Langmuir Monolayers

Drops of the PSI solution were carefully deposited with aid of a Hamilton syringe onto the surface of a 5 mM phosphate buffer solution serving as subphase. After an equilibration time was allowed for self-organization of the PSI complexes suspended at the air/water interface, the barriers were compressed at a constant speed (10 mm min^{-1}), while recording the corresponding π-A isotherm. After a certain surface pressure was reached indicating the formation of a compact monolayer (i.e., 42 mN m^{-1}), the monolayer was transferred to the electrode surface by pulling or dipping the substrate at a constant speed of 5 mm min^{-1}. The surface pressure was maintained constant during transfer by compressing the barriers as necessary. This process was automatically controlled by a software feedback, monitoring the interfacial tension at the air/liquid interface with the incorporated Wilhelmy plate.

Transfer by pulling

Before starting the experiment, the substrate was immersed into the subphase. After PSI deposition and compression, the monolayer was transferred by pulling the substrate out of the solution.

Transfer by dipping

The substrate was initially placed on top of the subphase surface. After PSI deposition and compression, the monolayer was transferred by dipping the substrate into the solution. After the procedure was finished, a copious amount of the superficial solution was carefully discarded in order to remove all remaining PSI. Finally, the modified substrate was taken out of the solution and used for further experiments.

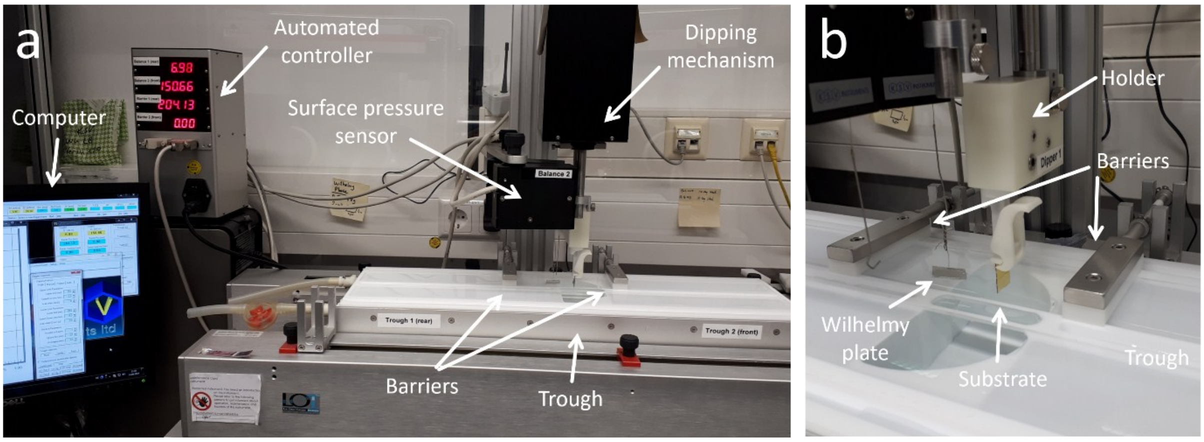

Fig. S3. Photograph of the experimental setup used for transfer of Langmuir monolayers onto the electrode surface by dipping or pulling the substrate during transfer. a) Complete setup highlighting the main elements. b) Magnification of the central part depicting the substrate holder and the position of the Wilhelmy plate used for surface tension monitoring.

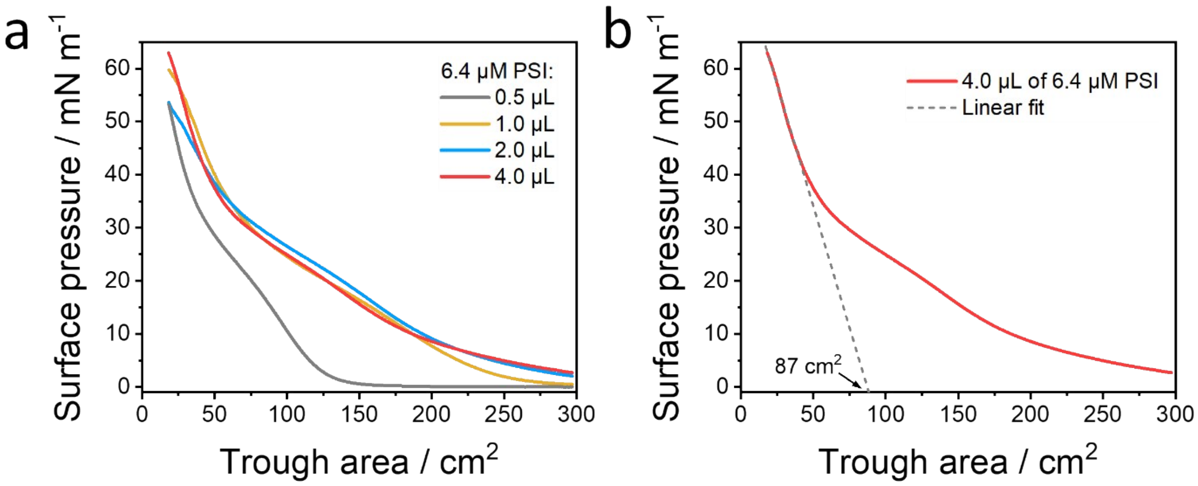

Fig. S4. Compression isotherms for Langmuir-Blodgett deposition of PSI trimer films. a) Comparison of π-A curves obtained for different amounts of PSI spread onto the air/water interface. Subphase: 5 mM phosphate buffer pH 7.0 at 20 °C. b) Fit for the linear region of the isotherm and extrapolation to zero surface pressure to estimate the limiting area. The mean molecular area estimated from the fitting was 565 nm^2.

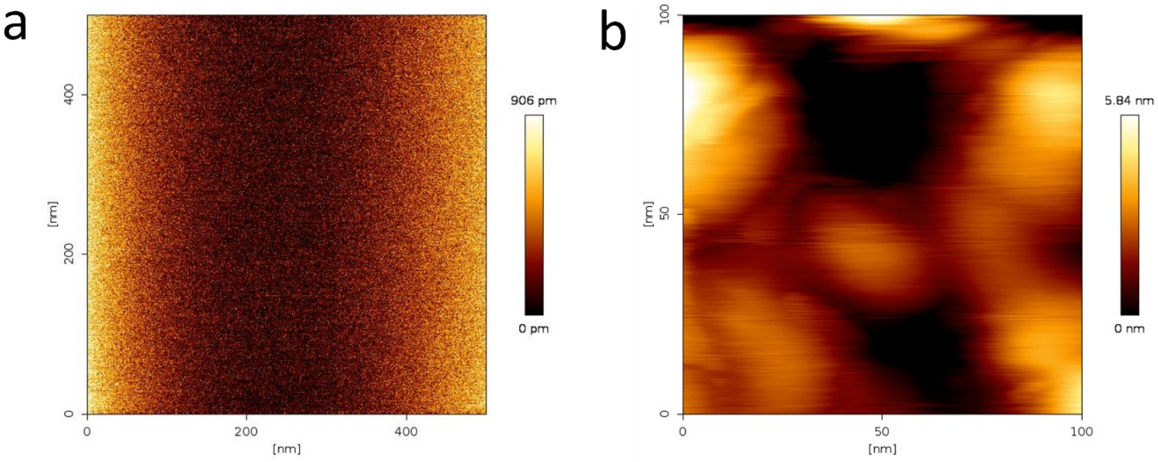

Fig. S5. AFM height profile characterization. a) Bare mica substrate. b) Assembled PSI film deposited on a mica substrate at a surface pressure of 42 mN m^{-1}. Transfer using vertical pulling at 5 mm min^{-1}.

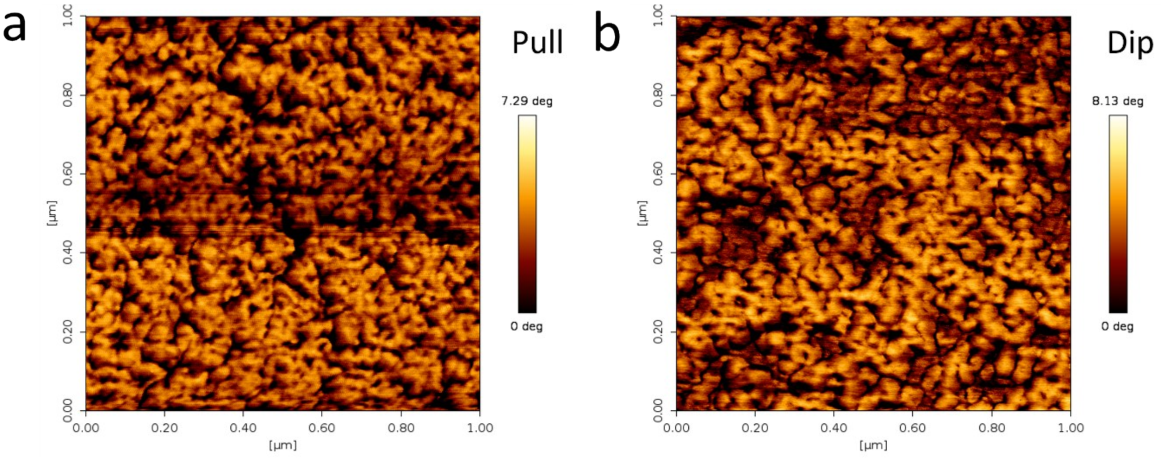

Fig. S6. AFM phase images of assembled PSI films deposited on a mica substrate at a surface pressure of 42 mN m^{-1}. a) Transfer using vertical pulling at 5 mm min^{-1}. b) Transfer using vertical dipping at 5 mm min^{-1}.

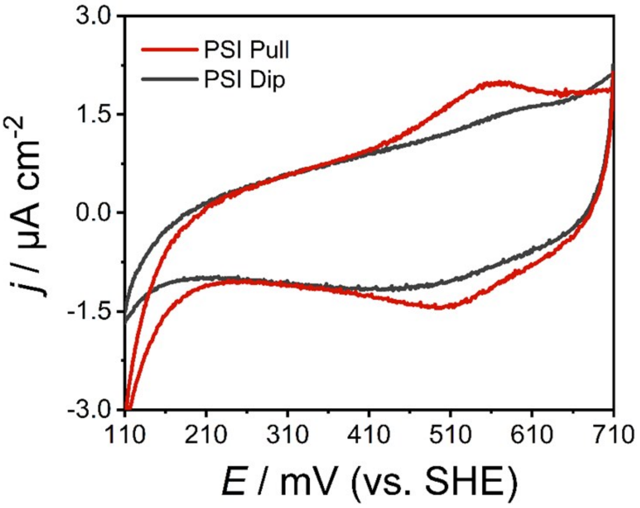

Fig. S7. Cyclic voltammograms in the dark of PSI-LB monolayers deposited on Au wafer either by pulling (red trace) or dipping (black trace) the substrate during transfer. Electrolyte: 2 mM MV^{2+} in 150 mM phosphate-citrate buffer pH 4.0. Scan rate: 10 mV s^{-1}.

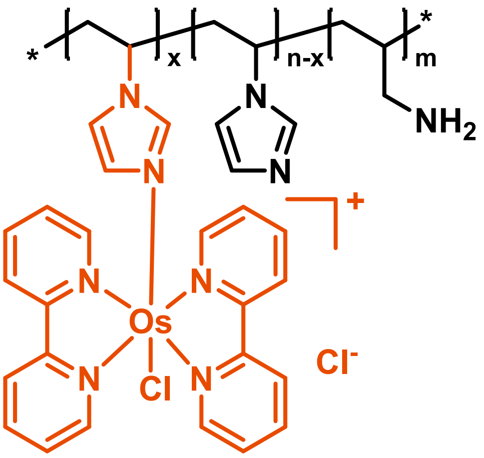

Fig. S8. Chemical structure of the redox polymer poly(1-vinylimidazole-*co*-allylamine)-[Os(2,2’-bipyridine)$_2$Cl]Cl.

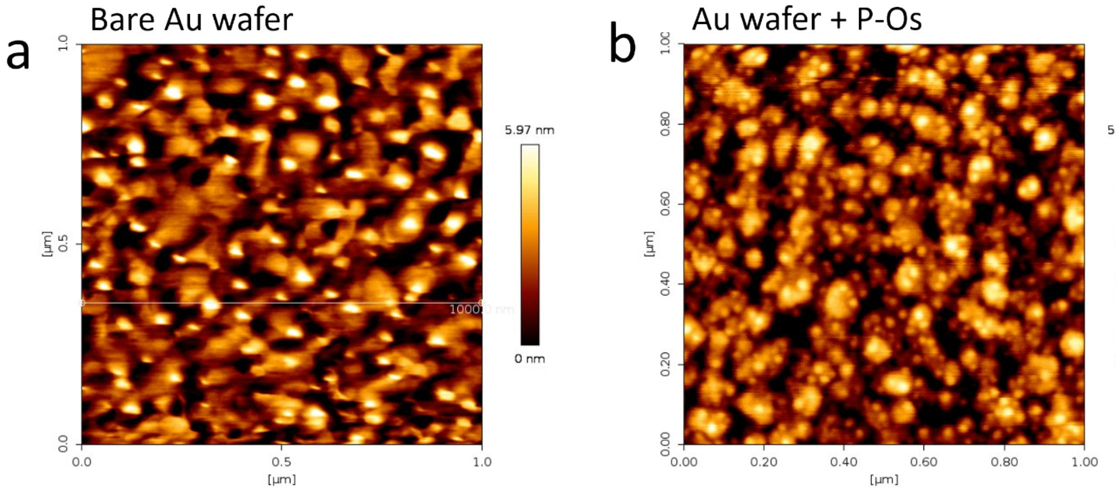

Fig. S9. AFM topography profiles. a) Bare Au wafer. b) Au wafer modified with a thin P-Os(I) film.

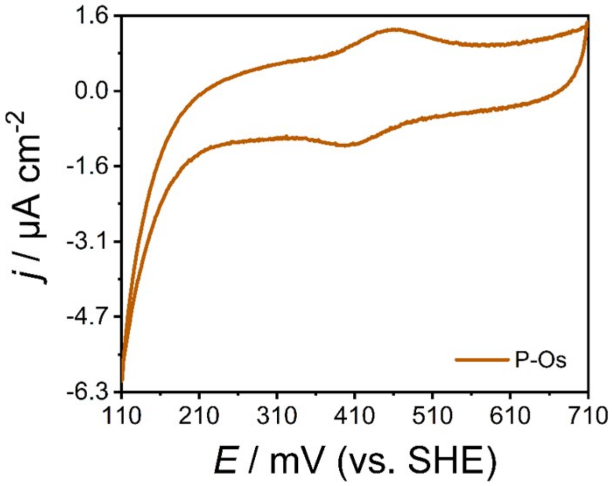

Fig. S10. Cyclic voltammogram for a thin film of P-Os(I) deposited on Au wafer. Electrolyte: 150 mM phosphate-citrate buffer pH 4.0. Scan rate: 10 mV s^{-1}.

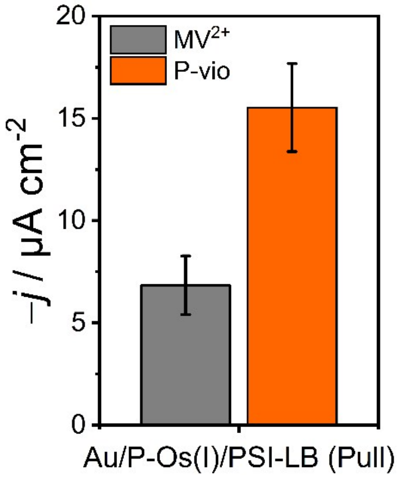

Fig. S11. Average values ($n = 3$ different electrodes) of photochronoamperometric responses obtained for Au/P-Os(I)/PSI-LB electrodes with MV^{2+} in solution or modified with P-vio as shown in Fig. 4 (main text). Error bars indicate standard deviation.

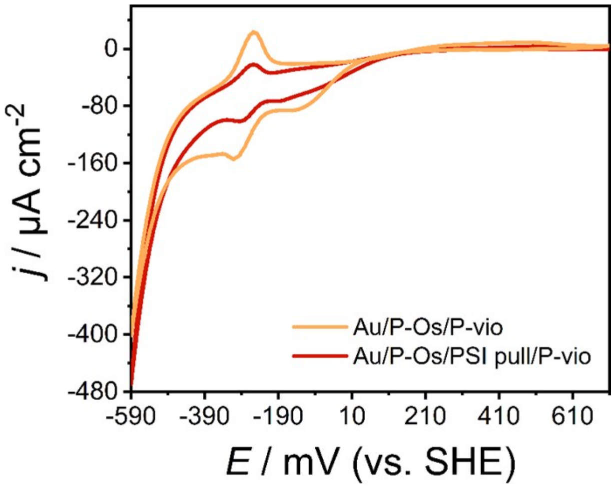

Fig. S12. Cyclic voltammograms for films of viologen modified polymer (P-vio) deposited as top layer over Au electrodes modified with P-Os(I) in the presence or absence of a PSI-LB transferred monolayer. CVs in dark. Scan rate: 10 mV s^{-1}. Electrolyte: air-equilibrated 150 mM phosphate-citrate buffer pH 4.0.

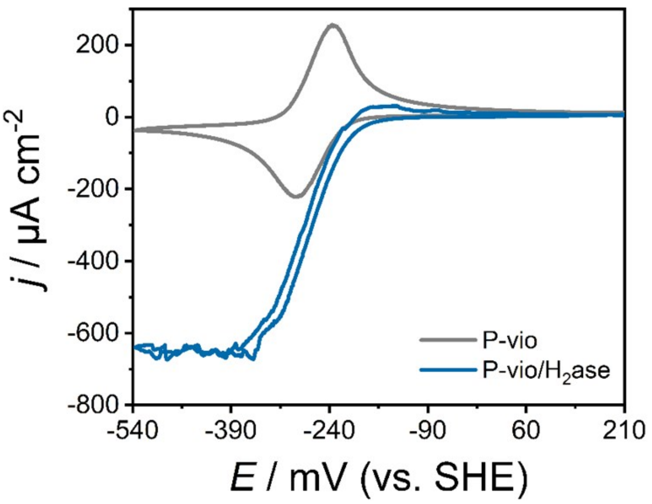

Fig. S13. Cyclic voltammograms for films of P-vio and the enzyme *Dv*H-[NiFeSe]-H_2ase embedded in P-vio deposited on glassy carbon electrodes (Ø = 3 mm). Electrolyte: Ar-saturated 150 mM phosphate-citrate buffer pH 4.0. Scan rate: 10 mV s^{-1}.

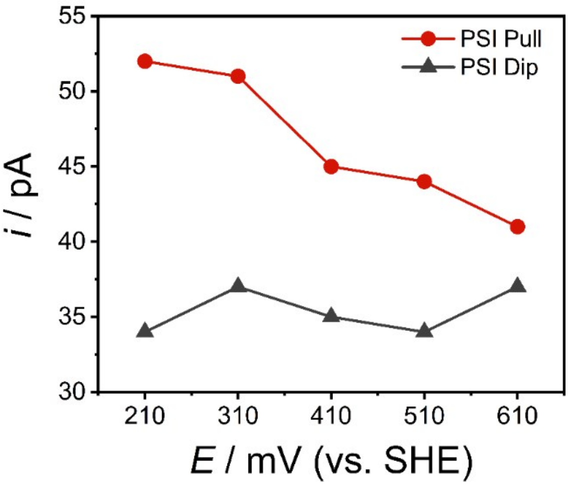

Fig. S14. Currents recorded with a Pt microelectrode (Ø = 25 µm) placed on top of Au wafers modified with PSI-LB/P-vio/H_2ase at different applied potentials and upon irradiation of the modified surface for the collection of generated H_2. Comparison for electrodes prepared after transfer of the PSI monolayer by pulling (red data points) or dipping (grey data points). E_{Tip} = 510 mV vs. SHE. Local irradiation through the microelectrode using white light (incident power: 280 mW cm^{-2}). Electrolyte: Ar-saturated 150 mM phosphate-citrate buffer pH 4.0.

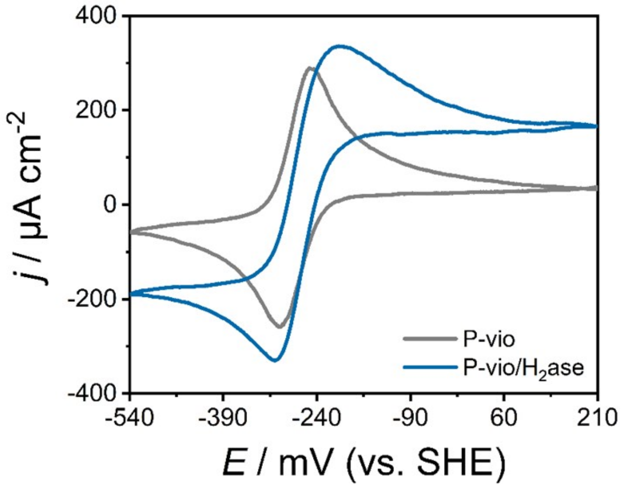

Fig. S15. Cyclic voltammograms for films of pristine viologen modified polymer (P-vio) and *Dv*H-[NiFeSe]-H_2ase embedded in P-vio both deposited on glassy carbon electrodes (Ø = 3 mm). Scan rate: 10 mV s^{-1}. Electrolyte: 150 mM phosphate-citrate buffer pH 5.0 saturated with a gas mixture of 5% H_2 in Ar.

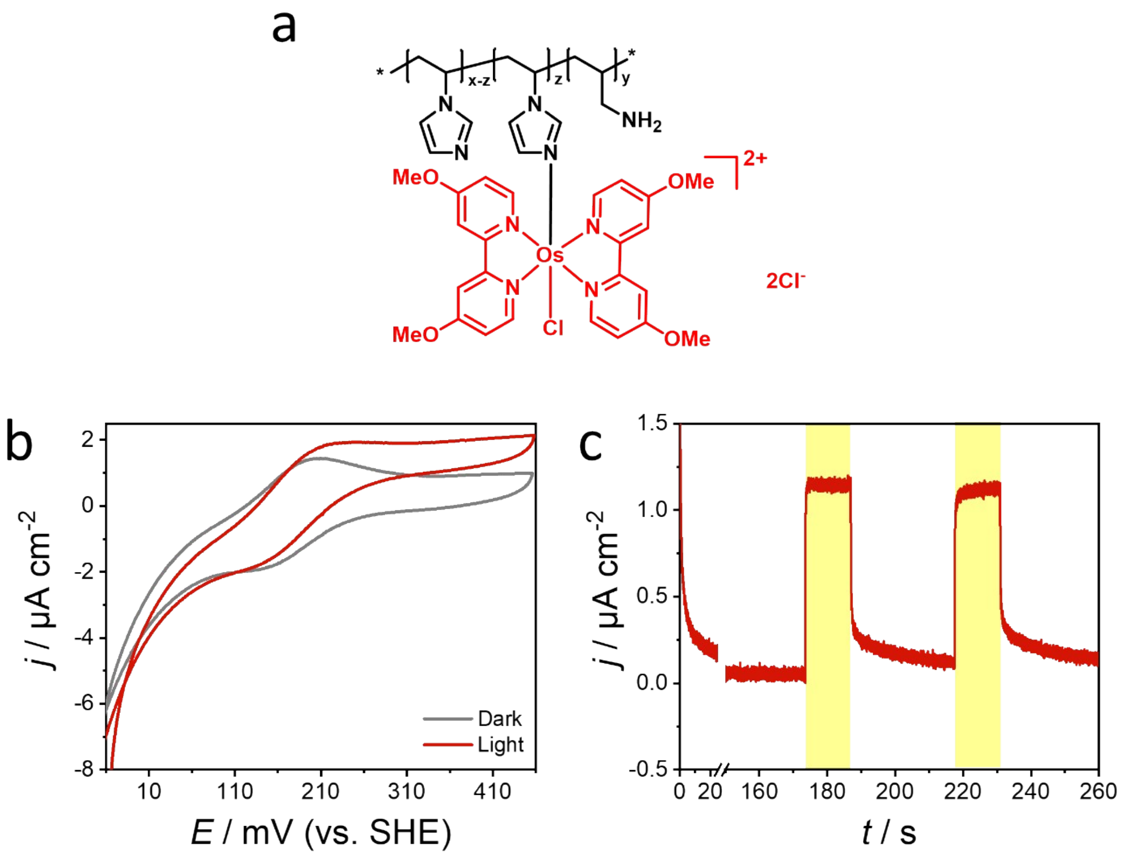

Fig. S16. a) Chemical structure of the low potential Os-complex modified redox polymer (P-Os(II): poly(1-vinylimidazole-*co*-allylamine)-[Os(dmxy-bpy)$_2$Cl]Cl_2). A PSII-based photoanode consisting of PSII embedded in P-Os(II) over a Au wafer electrode was characterized electrochemically by means of b) cyclic voltammetry and c) photochronoamperometric measurements. For (b) scan rate: 10 mV s^{-1}. For (c) E_{app} = 360 mV vs. SHE. Irradiation using red light ($\lambda > 600$ nm, incident power: 46 mW cm^{-2}). Electrolyte: air-equilibrated 50 mM MES buffer pH 6.5.

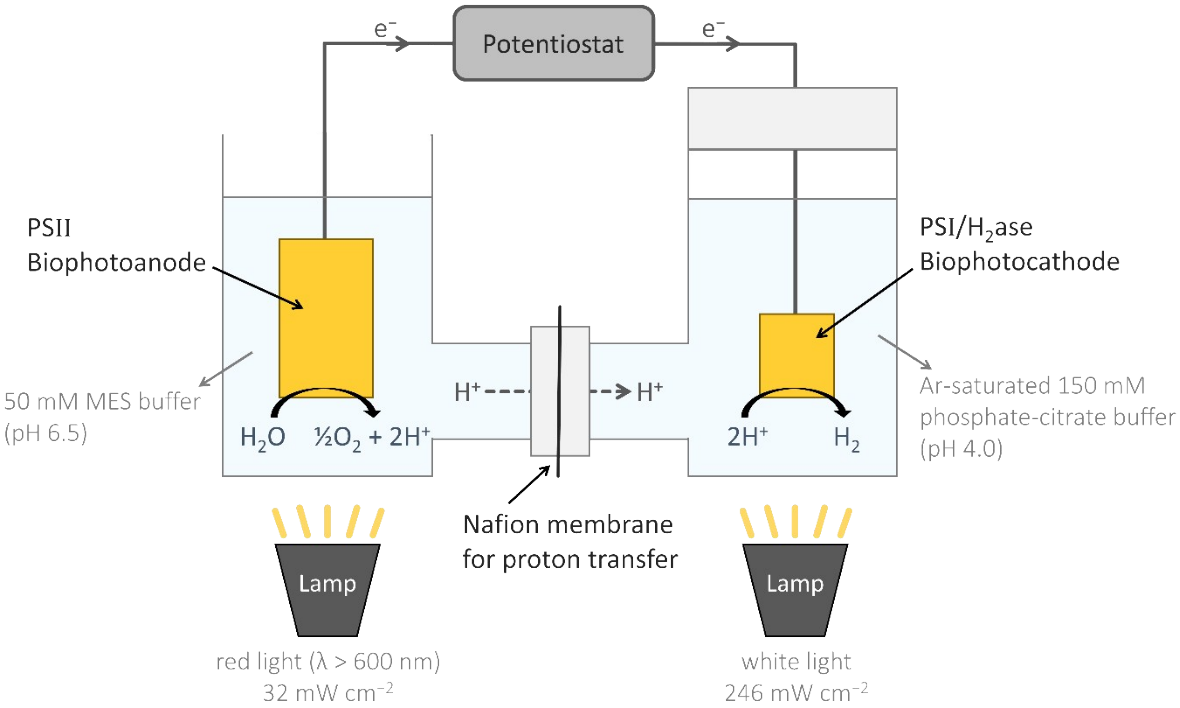

Fig. S17. Detailed schematic representation of the semi-artificial biophotovoltaic cell for bias-free water splitting, consisting of a PSII-based photoanode (left) coupled to a PSI/H_2ase-based photocathode (right) that enables the light-induced generation of O_2 and H_2. An oversized anode was used to ensure that the PSI-based photocathode was the limiting electrode.

References to the Supplementary Information

1 A. Ruff, J. Szczesny, S. Zacarias, I. A. C. Pereira, N. Plumeré and W. Schuhmann, *ACS Energy Lett.*, 2017, **2**, 964–968.

2 E.-R. Janeček, U. Rauwald, J. del Barrio, M. Cziferszky and O. A. Scherman, *Macromol. Rapid Commun.*, 2013, **34**, 1547–1553.